Journal of Nuclear Materials 149 (1987) 1–6
North-Holland, Amsterdam

CREEP AND MICROSTRUCTURAL CHANGES IN DISPERSION HARDENED Ni–20% Cr–1% ThO_2 DURING PROTON IRRADIATION

P. JUNG and P.B. CHILSON

Institut für Festkörperforschung der Kernforschungsanlage Jülich, Assoziation Euratom – KfA, D-5170 Jülich, Fed. Rep. Germany

Received 16 January 1987; accepted 3 February 1987

Irradiation creep and microstructural changes were studied at 573 K in a 20% cold worked Ni–20% Cr–1% ThO_2 alloy under 6.2 MeV proton irradiation. The irradiation creep strength was in the range of values found for FeCrNi alloys and for solution- and precipitation-hardened nickel alloys. Displacement doses up to 0.35 dpa increase the dislocation density in the cold worked specimens but have no observable effect on the dispersed ThO_2 particles.

Resistivity changes were observed in annealed as well as in cold worked specimens during thermal aging and to a much higher degree during irradiation. Transmission electron microscopy studies were inconclusive whether this was caused by short range ordering or by precipitation of a second phase in the NiCr system.

1. Introduction

The excellent high temperature strength of dispersion strengthened austenitic [1] and ferritic [2] oxidation-resistant alloys has prompted investigations on their potential use as structural materials in advanced nuclear reactors [3]. Tensile strength and creep at elevated temperatures of thoria-strengthened NiCr alloys were investigated previously [1,4–7]. In the present paper their creep properties under proton irradiation are investigated and compared to the behaviour of other materials. Transmission electron microscopy (TEM) is used to study the influence of irradiation on dislocation structure and ThO_2-dispersion. Electrical resistivity measurements supply further information on microscopic changes in the specimens during thermal aging and irradiation.

2. Experimental details

Specimen material (Ni–20 wt% Cr–1 wt% ThO_2) was supplied by Battelle Corp., Ohio, in the form of 254 μm sheets. These were rolled to 50 μm with intermediate anneals of 1 h at 1325 K. Specimens were used in the annealed and in a 20% cold worked condition, respectively. In both cases the diameters of the homogeneously dispersed ThO_2 particles ranged from about 5 to 100 nm [4]. The specimens were irradiated with protons which simulate fairly well mechanical property changes [8] as well as creep behaviour [9] under neutron irradiation. The proton energy on the front side of the specimen was 6.2 MeV, the atomic displacement rates were about 3×10^{-6} dpa/s [10] and the accumulated doses were 0.125 dpa and 0.35 pa, respectively.

The experimental set up and details of the irradiation procedure are described in ref. [11]. Irradiations were performed at the Jülich compact cyclotron. Before irradiation the specimens were held at temperature and stress to exhaust transient thermal creep. In contrast to irradiation creep experiments on austenitic stainless steels and other solution-hardened Ni alloys, it was not possible to keep the temperature of the NiCr–ThO_2 specimens sufficiently constant during irradiation by controlling the electrical resistivity. This was due to the low temperature dependence of the resistivity and to resistivity changes during irradiation. Therefore the temperature of the center part of the specimens was controlled by an infrared pyrometer to about ± 1 K and precise length and resistivity measurements were performed at 296 ± 0.1 K during beam shut-offs. The irradiation temperature was 573 K and tensile stresses of 100, 175, 250 and 300 MPa were applied.

3. Results and discussion

Fig. 1 shows the resistivity of 20% cold worked and of annealed Ni–20% Cr–1% ThO_2 specimens as a func-

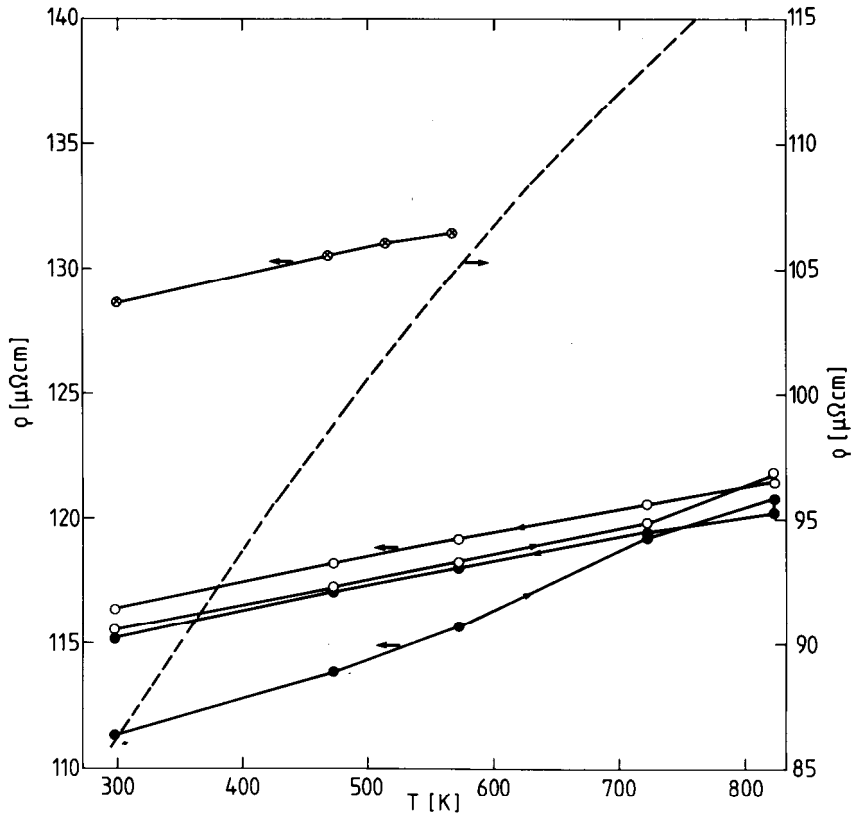

Fig. 1. Electrical resistivity as a function of temperature of annealed (○) and of 20% c.w. Ni–20% Cr–1% ThO_2 before (●) and after (⊗) irradiation at 573 K to 0.125 dpa. For comparison the resistivity of AISI 316 stainless steel is included (– – –).

tion of temperature. In contrast to solution-hardened Ni alloys and austenitic stainless steels (a curve of AISI 316 stainless steel is shown for comparison), the resistivity of the present alloy has a very small temperature dependence. During heating the resistivity shows a change of slope at about 600 K which is stronger in the 20% c.w. material. Holding the specimens at 823 K causes a slight decrease while holding for 12 h at 573 K has no noticeable effect. Anomalies of electrical resistivity have been observed in other NiCr alloys previously [12] and were tentatively explained by short range ordering. After irradiation to 0.12 dpa the resistivity is significantly increased but the temperature dependence is unchanged.

In fig. 2 the evolution of electrical resistivity during thermal aging and irradiation is compared. In both cases the measurements were performed at room temperature and a very steep increase was observed already during the first minutes of aging or irradiation, respectively. This initial increase in resistivity could not be monitored in detail as it occurred during the period of temperature stabilisation in the aging experiments and during beam adjustment in the irradiation experiments, respectively. It also partially invalidated measurements of resistivity changes at the aging temperature, as the starting values ρ_0 could not be measured with sufficient accuracy. Those measurements give curves which are similar in shape to those in fig. 2 but vary in their absolute position due to the uncertainties in ρ_0. After the initial increase, the resistivity declines gradually. Annealed specimens show a similar behaviour during thermal aging as cold worked material, apart from a slightly higher value of ρ_0 and a higher initial increase of the resistivity (fig. 2).

The thermal aging experiments were performed at zero stress. The irradiations were performed at various stresses as indicated, while the measurements at room temperature were always performed at 250 MPa. Obviously, stress changes in both directions cause small increases in resistivity. This makes the evaluation of a

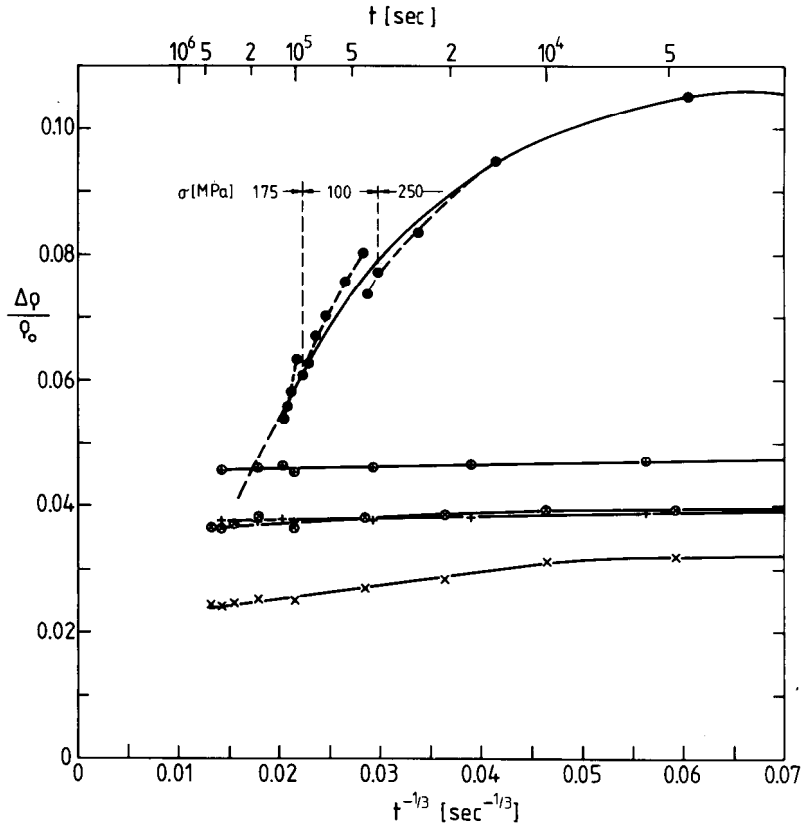

Fig. 2. Relative change of electrical resistivity of 20% c.w. Ni–20% Cr–1% ThO_2 during irradiation at 3×10^{-6} dpa/s at 573 K (● and during thermal aging at 823 K (×) and 863 K (+), respectively. Symbols ⊗ and ⊕ indicate thermal aging of annealed specimens at 823 K and 863 K, respectively. Resistivity measurements were always at room temperature.

time law rather uncertain. An asymptotic $t^{-1/3}$ behaviour of resistivity as suggested by the plot in fig. 2 would be expected for diffusion-controlled coarsening of precipitates [13] due to the reduction of the concentration of atoms in solution [14,15]. Such a $t^{-1/3}$ law of the resistivity could be clearly established in Ni(Al) alloys during irradiation as well as during thermal aging [16]. For the present material an unambiguous evaluation of a time law is much more difficult due to the small changes during thermal aging and due to the limited irradiation time, respectively.

The stress dependence of the electrical resistance,

$$\frac{\Delta R/\Delta\sigma}{R_0} = \frac{\Delta\rho/\Delta\sigma}{\rho_0} + \frac{1+2\nu}{Y}$$

(ν = Poisson's ratio, Y = Youngs modulus), was about 9×10^{-6}/MPa which can almost entirely be ascribed to elastic changes of specimen geometry, given by the second term. That means that stress effects on resistivity (first term) are negligible.

Fig. 3 shows the plastic strain $\Delta l/l_0$ of 20% c.w. NiCr–1% ThO_2 during irradiation at 573 K as a function of displacement dose. After starting the irradiation a contraction of the specimen against the applied stress occurs. But already after a dose of 0.01 dpa, creep in the stress direction is observed at a gradually decreasing creep rate, which becomes constant around 0.1 dpa. Stress changes cause transient strains similar to observations in other materials [9]. Measurements of Youngs modulus Y showed no change during irradiation, indicating that elastic contributions to the irradiation induced length change are negligible.

In fig. 4 irradiation creep rates ($\dot{\epsilon}$) per displacement rate (K) of the 20% cold worked NiCr–ThO_2 alloy are compared to results from other materials. Obviously the irradiation creep rates of the dispersion strengthened

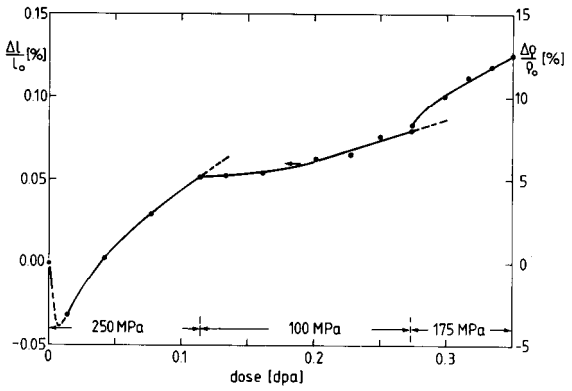

Fig. 3. Irradiation creep stain of 20% c.w. Ni–20% Cr–1% ThO_2 during irradiation at 573 K as a function of dose and tensile stresses as indicated.

alloy coincide closely with those of solution-hardened and precipitation hardened aloys at low stresses. That means the dispersed particles which give the material its superior thermal creep strength at high temperatures do not contribute to the irradiation creep strength. In contrast to the other Ni alloys, no deviation from the linear stress dependence is observed in the NiCr–ThO_2 alloy at stresses up to 300 MPa. This does not exclude a higher stress dependence at still higher stresses. For example, in AISI 316 stainless steel a higher than linear

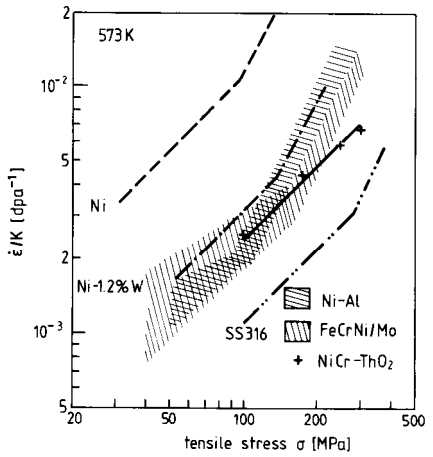

Fig. 4. Irradiation creep rates $\dot{\epsilon}$ per displacement rate K of Ni–20% Cr–1% ThO_2 (+) at 573 K as a function of tensile stress. The curves indicate results from other 20% cold worked materials: pure Ni (– – –), Ni–1.2 at% W (–·–). AISI 316 stainless steel (– – ··), and ranges of Ni(Al) and FeCrNi/FeCrNiMo alloys as indicated by the shaded areas.

stress dependence is observed only beyond 250 MPa.

TEM observations show that the original dislocation structure which indicates some cell structure becomes slightly more dense and more homogeneous after irradiation. The dispersed ThO_2-particles are visible by bright-field imaging (fig. 5a) as well as in dark field (fig. 5b) by using the small extra diffraction spots outside the matrix spots (fig. 5c). These spots stem from individual ThO_2 particles and are largely aligned on rings corresponding to the cubic ThO_2 structure ($a = 0.560$ nm). In bright field ThO_2 particles of 5 to 100 nm are visible in agreement with ref. [4], while the dark field reveals only part of this distribution – according to the spots used for imaging. The diffuse diffraction rings around the central spot are caused by hexagonal NiO ($a = 0.2954$ nm, $c = 0.7236$ nm). Dark field images (fig. 5d) using parts of these rings showed very small oxide crystals (≈ 4 nm). Stereo-microscopy indicated that these oxides are distributed throughout the bulk of the material with some enhancement along dislocation lines. The oxide rings became more intense by aging even in vacuum better than 10^{-3} Pa. Irradiation has no perceivable effect on distribution and morphology neither of the ThO_2 nor the NiO particles.

In a previous work [17] a change in the morphology of the thoria particles in a similar alloy was observed after 5 MeV Ni^{++} irradiation at temperatures between 798 and 1023 K to doses of 50 dpa at $K = 3 \times 10^{-2}$ dpa/s. In that study the matrix–particle interface became irregular and a shell of new thoria particles formed around the original ones. In the present investigation no such modifications of the original particles could be detected. This may be due to the much smaller accumulated doses or due to the lower temperature in the present study. But most probably it is due to the much lower recoil energies transferred by the protons.

In fig. 6 functions $W_d(T_c)$ are plotted which describe [10] the fraction of *displaced atoms* which are produced in cascades of initial energies *below* T_c. The corresponding number ν_c of displaced atoms in a cascade which is initiated by an energy transfer T_c to the primary atom is given on the upper abscissa. Calculations are given for 6.2 MeV protons and for 5 MeV Ni ions. The calculations show that during the Ni irradiation the defects originate from cascades which are on the average more than one order of magnitude more energetic than those produced by the protons. The calculations did not include degradation of the particle energy. Therefore a calculation for 0.5 MeV Ni ions is included which shows that during slowing down the displacement spectrum does not weaken considerably.

The second set of curves of fig. 6 compares the

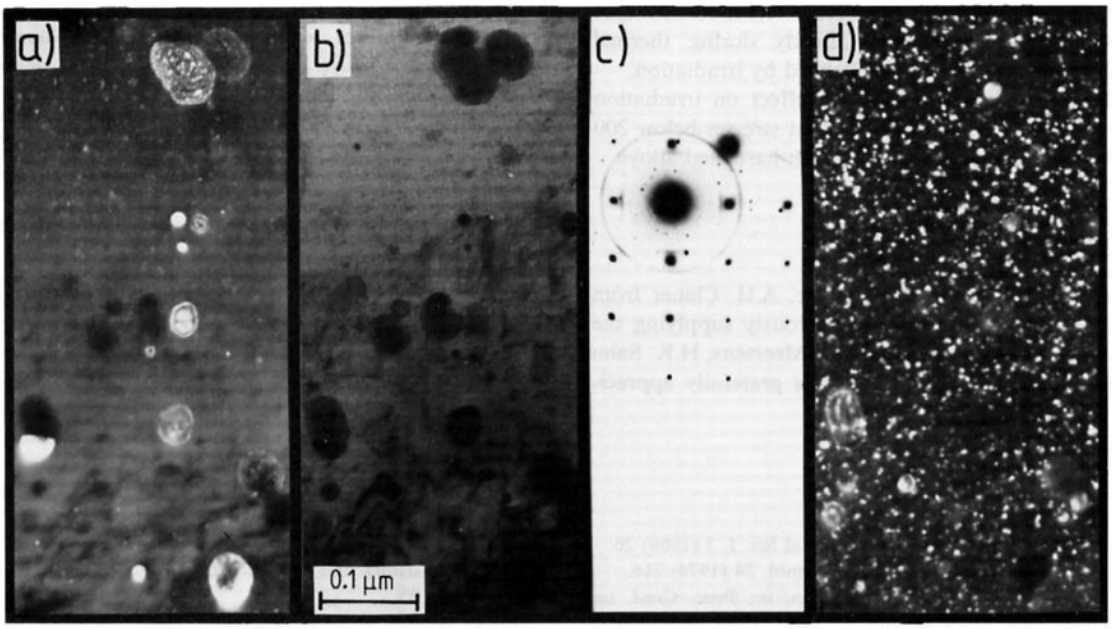

Fig. 5. Bright (a) and dark (b, d) field images of Ni–20% Cr–1% ThO_2. The dark field images are obtained by using the small extra spots (b) and the diffuse rings (d) of the diffraction picture (c), respectively.

fraction of *primary events* $(1 - W_c)$ with recoil energies *above* T_c. The visibility limit for defect clusters in the TEM presumably lies in the range of some twenty defects. The fraction of cascades with more than 30 defects is almost an order of magnitude higher for 5 MeV Ni irradiation compared to 6.2 MeV protons, and by less than 0.1% of the primary events cascades of $\nu_c > 40$ defects are produced by 6.2 MeV protons. This level of 0.1% is reached by the 5 MeV Ni ion only at $\nu_c > 300$ defects. In a Ni(Al) precipitation-hardening alloy, doses below 0.1 dpa already caused strong irradiation-induced precipitation and redistribution of preexisting precipitates [16]. The reason for the much lower sensitivity to irradiation of the ThO_2 particles compared to the γ' in Ni(Al) is probably the much lower solubility of thorium in nickel. We therefore assume that the ThO_2 particles are only affected by some kind of recoil mixing, while the effect of irradiation on precipitation in the NiAl system is predominantly by long range diffusion involving some coupling of the solute Al to point defects.

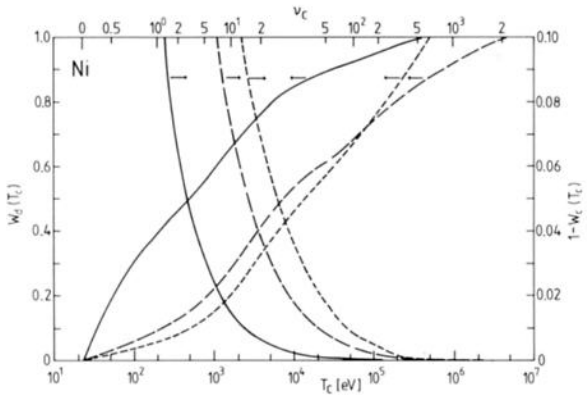

Fig. 6. Fraction W_d of displaced atoms in Ni produced in cascades of primary energies above T_c during irradiation with 6.2 MeV protons (———) and Ni ion of 0.5 (– – –)– and 5 MeV (— —), respectively. Included are curves $(1 - W_c)$ which give the fraction of primary events (cascades) above a certain energy T_c. The upper abscissa indicates the number ν_c of displacements in a cascade of primary energy T_c.

4. Conclusions

(1) Irradiation of 20% cold worked Ni–20% Cr–1% ThO_2 by 6.2 MeV protons to doses up to 0.35 dpa has a small effect on the dislocation structure, but no measurable influence on the morphology or distribution of the dispersed ThO_2 particles.

(2) A clear change in electrical resistivity indicates some atomistic rearrangement already during thermal aging which is strongly enhanced by irradiation.
(3) The ThO_2 dispersion has no effect on irradiation creep strength of this material at stresses below 200 MPa when compared to solution hardened alloys.

Acknowledgements

The authors are indebted to Dr. A.H. Clauer from Battelle Columbus Labs. for generously supplying the material. The assistance of Ms. D. Meertens, H.K. Sahu and H. Klein in the TEM work is gratefully appreciated.

References

[1] B.A. Wilcox and A.H. Clauer, Metal Sci. J. 3 (1969) 26.
[2] J.J. Huet and V. Leroy, Nucl. Technol. 24 (1974) 216.
[3] M. Snykers and V. Vandermeulen, in: Proc. Conf. on Dimensional Stability and L. Proc. Conf. Mechanical Behaviour of Irradiated Metals and Alloys, Brighton, UK, 1983 (British Nuclear Energy Society, London, 1983) p. 91.
[4] B.A. Wilcox and A.H. Clauer, Acta Metall. 20 (1972) 743.
[5] D.H. Killpatrick, in: Proc. 2nd Int. conf. on Strength of Metals and Alloys, Pacific Grove, USA (American Society for Metals, 1970) p. 649.
[6] M.J.H. Ruscoe, L.F. Norris, M.A. Clegg and D.J.I. Evans, in: Proc. 3rd Int. Conf. on Strength of Metals and Alloys, Cambridge, UK (The Institute of Metals and The Iron and Steel Institute, 1973) p. 96.
[7] J.E. Franklin, G. Judd and G.S. Ansell, ibid. ref. [6], p. 345.
[8] R.J. Jones, D.L. Styris and E.R. Bradley, in: Effects of Radiation on Structural Materials, ASTM-STP 683 (1978) 346.
[9] P. Jung, J. Nucl. Mater. 113 (1983) 133.
[10] P. Jung, J. Nucl. Mater. 117 (1983) 70. Report KfA Jül-1823 (1983) ISSN 0366-0885
[11] P. Jung, H.K. Sahu and A. Schwarz, Nucl. Instr. and Meth. A234 (1985) 331.
[12] H.E. McCoy, Jr. and D.L. McElroy, Trans. ASM 61 (1968) 730.
[13] K. Binder and D. Stauffer, Z. Physik B24 (1976) 407.
[14] I.M. Lifshitz and V.V. Slyozov, J. Phys. Chem. Sol. 19 (1961) 35.
[15] C. Wagner, Z. Elektrochemie 65 (1961) 581.
[16] P. Jung, M.I. Ansari, H. Klein and D. Meertens, J. Nucl. Mater. 148 (1987) 148.
[17] R.H. Jones, J. Nucl. Mater. 74 (1978) 163.